Available online at www.sciencedirect.com
ScienceDirect
Tetrahedron
Tetrahedron 64 (2008) 1860–1867
www.elsevier.com/locate/tet

Synthesis and properties of iridium complexes based 1,3,4-oxadiazoles derivatives

Zhaowu Xu [a], Yang Li [a], Xuemei Ma [a], Xindong Gao [b], He Tian [a,*]

[a] *Key Laboratory for Advance Materials and Institute of Fine Chemicals, East China University of Science and Technology, Shanghai, 200237, China*
[b] *State Key Laboratory on Surface Physics, Fudan University, Shanghai 200433, China*

Received 29 September 2007; received in revised form 26 November 2007; accepted 28 November 2007
Available online 4 December 2007

Abstract

A series of iridium complexes with 2,5-diaryl-[1,3,4]-oxadiazole ligands were synthesized and their electrochemical, photophysical, and electroluminescent (EL) properties studied. It was found that electron-withdrawing or donating substituents on the phenyl ring affected the emission maxima. Complex **3**, iridium(III) bis(2,5-bis-(2-hydroxyphenyl)-[1,3,4]oxadiazolato-$C^{2\prime},N^{3}$) (acetyl acetonate), was characterized by single-crystal X-ray structural determination. Three organic light emitting diodes devices were fabricated, which showed stable green-yellow luminescence.

1. Introduction

Organic light emitting diodes (OLEDs) have attracted a great deal of interest due to their potential application in flat displays.[1] Particularly, phosphorescent materials like iridium(III) complexes have received considerable attention because of their high phosphorescence quantum efficiency, which is due to mixing the singlet and the triplet excited states via spin-orbit coupling and enhancing the triplet-state subsequently.[2–4] The research on iridium complexes as well as their application in OLEDs are mainly focused on designing new and facile ligands. Based on (*iso*) quinoline, pyrazine, pyrimidine, pyridine, and pyrazole derivatives, several OLEDs with efficient blue, green, and red emission iridium(III) phosphorescence were fabricated.[5]

Recently, some heteroleptic iridium(III) complexes based on fluorinated 1,3,4-oxadiazole were reported, which could be tuned to blue by dithiolate ancillary ligands.[6]1,3,4-Oxadiazole derivatives are one of the most widely studied classes of electron-injection/hole-blocking materials due to their electron deficiency, high photoluminescence quantum yield, good thermal, and chemical stabilities. It has been shown previously that 2-(4-biphenylyl)-5-(4-tertbutylphenyl)-[1,3,4]-oxadiazole (PBD) functions very well as an excellent electron-transport material (ETM) in multilayer OLEDs.[7]

In this paper, we designed and synthesized a series of iridium-(III)–oxadiazole complexes as emitting materials. The ligands of iridium with different substituents show different electronic properties, which can be expected to synthesize color tunable emissive iridium complexes. Subsequently, we expected to increase the understanding of the structure–property relationship of these iridium complexes better. Finally, the usefulness of three complexes as triplet emitters in electroluminescent devices was examined by applying them as guests in CBP hosts in two different multilayered device architectures. It is expected that incorporation of an electron-deficient oxadiazoles can increase the electron affinity and transporting properties of these complexes, which would lead to the reduction of driving voltage and the increase in energy conversion efficiency.

2. Results and discussion

Synthetic routes for the ligands and their iridium complexes are outlined in Scheme 1. 2-Aryl-5-alkyl-[1,3,4]-oxadiazoles

* Corresponding author. Fax: +86 21 64252288.
E-mail address: tianhe@ecust.edu.cn (H. Tian).

0040-4020/$ - see front matter © 2007 Elsevier Ltd. All rights reserved.
doi:10.1016/j.tet.2007.11.099

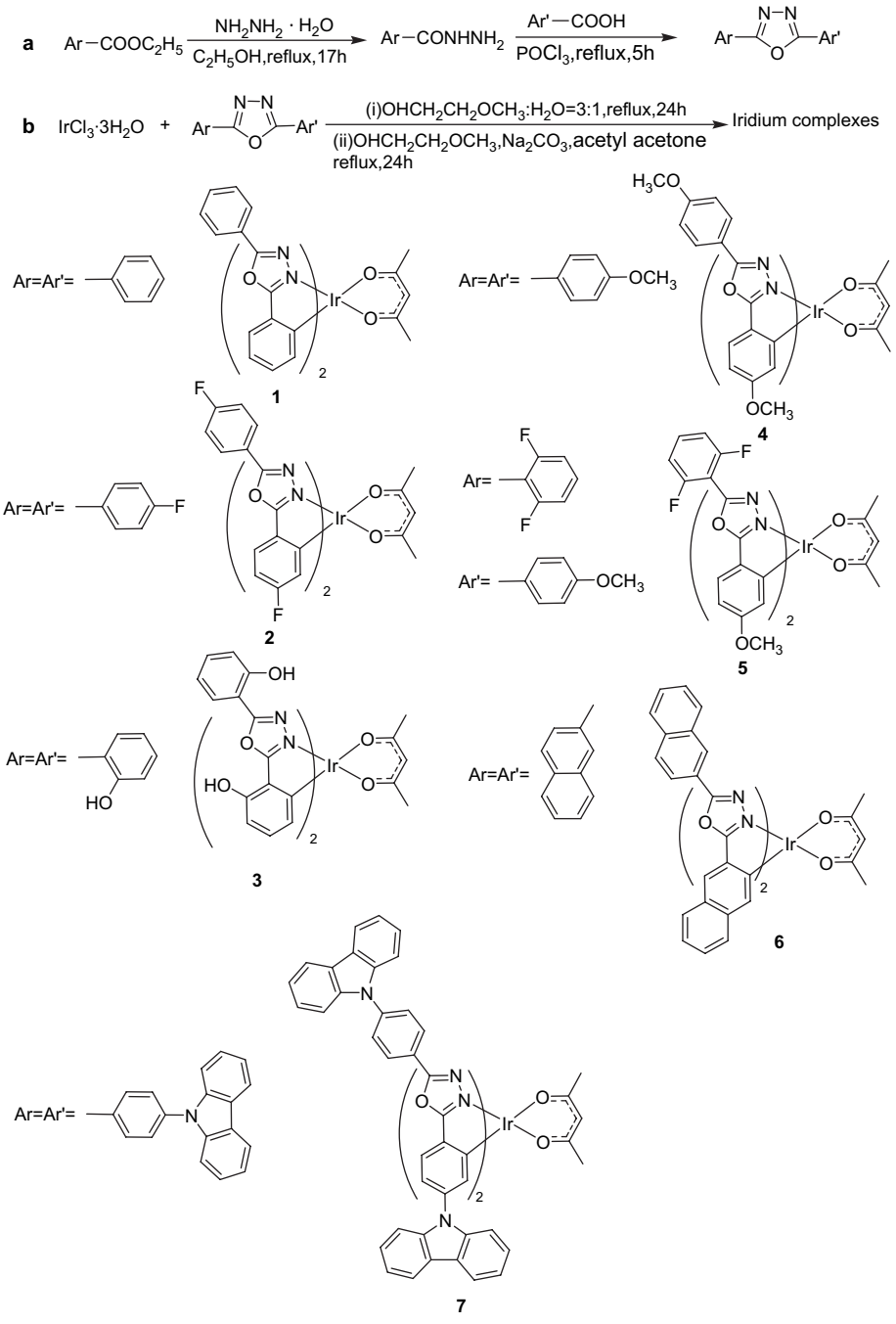

Scheme 1. Synthesis of Ir–OXD complexes.

were so unstable under the cyclometalated reaction condition used that did not yield the desired iridium complexes. The synthetic method used to prepare these complexes involves two steps. In the first step, $IrCl_3 \cdot 3H_2O$ was allowed to react with an excess of the cyclometalated ligands (2.5×) to give a chloride-bridged dinuclear complexes, i.e., $(x\text{OXD})_2Ir_2(\mu\text{-}Cl)_2(x\text{OXD})_2$. The chloride-bridged dinuclear complexes can be readily converted to emissive, mononuclear complexes $(x\text{OXD})_2\text{Ir(acac)}$ by replacing the two bridging chlorides with bidentate acetyl acetonate. These reactions result in $(x\text{OXD})_2\text{Ir(acac)}$ with a yield of 70–85%.

To have an insight into the highest occupied molecular orbital (HOMO) energy levels of the complexes, cyclic voltammetry experiments were carried out for all complexes. However, no reduction processes were observed in dichloromethane in the range of −2 to 2 V.[8] The oxidation potentials of all complexes were collected in Table 1. Figure 1 depicts the cyclic voltammetry of complex **1**, **2**, **4**, and **5** in CH_2Cl_2 solution at a 100 mV/s scan rate under argon atmosphere. The decreasing order of oxidation potential of the complexes has been observed in the following: **2** (4,4′-difluoro)>**5** (2,6-difluoro-4′-methoxyl)>**1** (unsubstituted)>**4** (4, 4′-dimethoxyl). This observation shows that different substituent groups can tune the electronic nature of these complexes. Complex **2** displays a significantly anodic shift (210 mV),

Table 1
Photophysical and electrochemical data for $(OXD)_2Ir(acac)$

Complex	Absorption λ (log ε)[a] (nm)	λ_{em}[b] (nm)	ΔE (eV)	Φ_{em}	E_{ox}[c] (V)
1, $(OXD)_2Ir(acac)$	267 (4.9), 289 (4.8), 415 (3.9)	524	2.4	0.41	1.24
2, $(dfOXD)_2Ir(acac)$	290 (4.8), 397 (3.8)	508	2.5	0.33	1.45
3, $(dhOXD)_2Ir(acac)$	266 (4.9), 293 (4.8), 410 (4.0)	516	2.4	0.12	1.24
4, $(dmOXD)_2Ir(acac)$	269 (4.8), 300 (4.9), 407 (3.9)	512	2.5	0.10	1.22
5, $(dfmOXD)_2Ir(acac)$	290 (4.8), 415 (3.8)	519	2.5	0.19	1.38
6, $(nOXD)_2Ir(acac)$	261 (4.9), 315 (4.6), 477 (3.2)	569	2.2	0.28	1.07
7, $(dcOXD)_2Ir(acac)$	290 (4.9), 344 (4.5), 445 (3.7)	536	2.4	0.65	1.44[d]

[a] Measured in THF solution.
[b] Measured in THF at 298 K excited at 340 nm. $(ppy)_2Ir(acac)$ was used as the reference for the quantum yield.
[c] Measured in CH_2Cl_2 at a concentration of 10^{-3} M and scan rate was 100 mV/s.
[d] Complex **7** has an reversible oxidation potential.

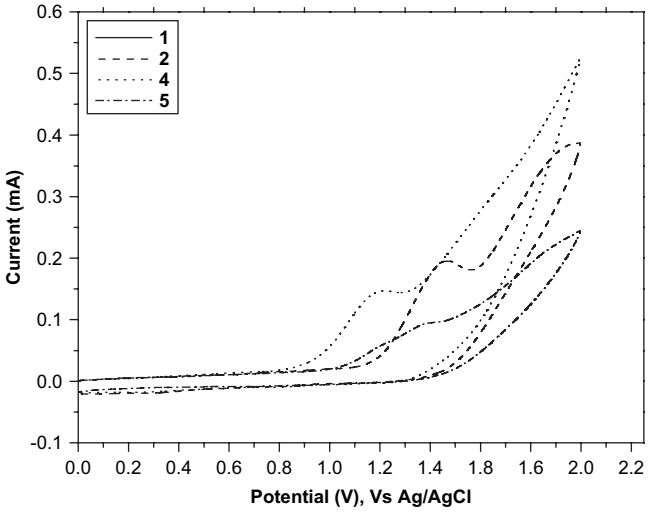

Figure 1. Cyclic voltammograms of complexes in 0.1 M n-Bu_4NClO_4 at a scan rate of 100 mV/s.

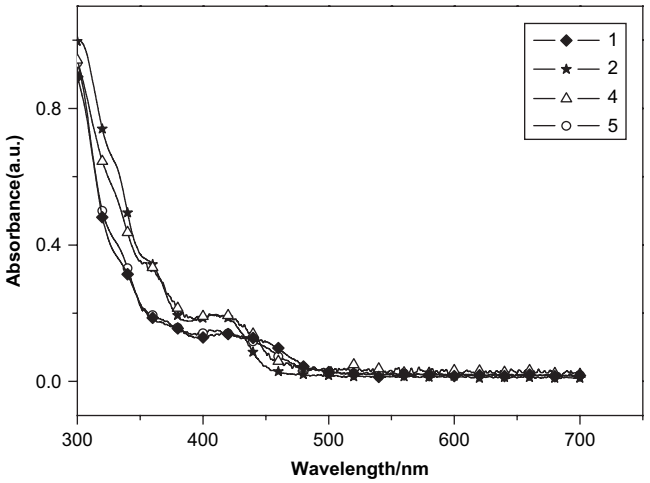

Figure 2. Absorption spectra of complexes **1**, **2**, **4**, and **5** in THF (1×10^{-5} M).

compared to the unsubstituted complex **1**. The fact indicated that electron-withdrawing groups can lower the HOMO energy levels effectively. However, the electron-donating substituent group, $-OCH_3$, does not affect the HOMO level effectively, as evidenced by the fact that the oxidation potential of complex **4** exhibits a slight lower ($\Delta E=-20$ mV) than that of complex **1**. Furthermore, it should be noted that the oxidation potential of complex **5**, which contains $-F$ and $-OCH_3$ together is in the middle of that of complex **2** and complex **4**.

The photophysical and electrochemical data of $(OXD)_2Ir(acac)$ complexes are collected in Table 1. Figure 2 shows the absorption spectra of complex **1**, **2**, **4**, and **5** as representative examples of this series of complexes. It is suggested that the bands observed in the ultraviolet part of the spectrum (250–350 nm) can be assigned to the allowed ligand-centered ($\pi-\pi^*$) transitions. Somewhat weaker, broad, and featureless absorption bands located in the lower part of energy ($\lambda_{max}>400$ nm) suggest that these bands are attributed to the coexistent spin-allowed metal-to-ligand charge transfer ^{1}MLCT and spin-forbidden ^{3}MLCT/$^3\pi-\pi^*$ transitions as result of the spin-orbit coupling of iridium(III) according to the bands position, size, and the extinction coefficients.[3a]

All of these complexes show strong luminescence in the THF solutions. Most of the complexes exhibit high solution phosphorescence quantum yields ($\Phi_p=0.1-0.65$). Additionally, large Stokes shift between the lowest energy absorption and emission bands and resolved vibronic structure of phosphorescent emission spectra suggested that these iridium–oxadiazole complexes mainly emit from $^3\pi-\pi^*$ transitions.

As shown in Figure 3, complex **6** showed a nearly 44 nm bathochromic emission shift as compared to that of complex

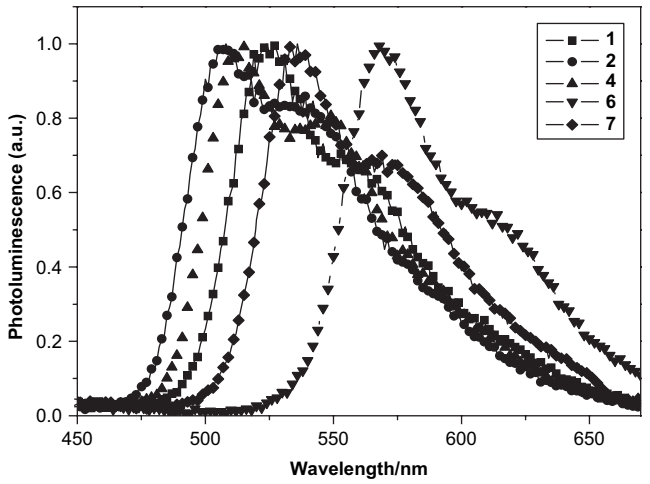

Figure 3. Normalized photoluminescence spectra of the complexes in THF (1×10^{-5} M).

1 owing to the π-system increasing effect. Apparently, the shift is smaller than that of ppy-based system of $Ir(ppy)_2(acac)$ and $Ir(NaPy)_2(acac)$ [NaPy=2-(1-naphthalenyl)pyridine] but similar with the pip-based system of $Ir(pip)_2(acac)$ and $Ir(Napip)_2(acac)$ [Napip=2-(1-naphthalenyl) imidazo[1,2-*a*]pyridine].[3] However, unlike the pipiridium system, the HOMO of complex **6** has remarkable change, which could be supported by the electrochemical data. This difference can be explained that the HOMO of these complexes are somewhat extended to the phenyl-π and Ir-d orbitals like revealed by the MO calculations of ppy-based complexes.

We still investigated the substituents attached to the phenyl rings, including electron-withdrawing and donating substituents. The emission maximum of complex **2** with fluorine atoms on the phenyl rings revealed a 16 nm blue shift with respect to that of the complex **1**, which is due to the increase of HOMO–LUMO gap. A similar blue shift was observed in the end-absorption of complex **1** and **2**. This observation is consistent with the research of Ir–ppy complexes. Introducing fluorine atoms to the phenyl rings would lower and stabilize the HOMO levels. Similarly, a blue shift of 12 nm of the emission maximum was observed by using electron-donating groups, $-OCH_3$, instead of fluorine atoms. This observation concerning the substitution effect is like the results in the iridium–phenylbenzthiazole system. Chen et al. revealed that the iridium–phenylbenzthiazole complexes with various substituents ($-F$, $-OCH_3$, $-CH_3$) exhibit shorter emission maxima than that of unsubstituted complex.[9] In addition, the emission maxima of complex **5** exhibits longer by 9 nm than that of complex **2** and shorter by 5 nm than that of complex **1**, which is consistent with the observation of electrochemical properties. It can be inferred that the photophysical properties of oxadiazoles based iridium complexes are mainly dependent on the properties of the phenyl ring iridium cyclometalated. Based on the discussion above, it is suggested that controlling the substituents on the phenyl may realize color emission tunable.[3b,3d]

It should be noted that converting the substituents with 4,4′-dicarbazole, the maximum emission peak of complex **7** shows a large bathochromic shift compared to the unsubstituted complex owing to electron-donating effect and increase of ligand π-system. Additionally, complex **7** exhibits the highest phosphorescent quantum efficiency in this series of complexes, up to 0.65. There may be mainly two reasons: one is the high efficiency of carbazole group, the other is sterically hindered effect.[10,11] We hope this fact would provide useful information on fabricating OLEDs devices.

Complex **3** has octahedral coordination geometry around Ir and has crystallographically imposed twofold symmetry, with the Ir atom lying on a twofold axis (shown in Fig. 4). The length of Ir–C bonds of the complex ((Ir–Cav) 1.996(5) Å) are shorter than that of Ir–N bonds ((Ir–Nav) 2.041(5) Å). The Ir–C bond length is similar to those in the analogous complexes reported. Furthermore, the Ir–N bond lengths also fall within the range of values for those of the reported complexes. The Ir–O bond lengths of 2.131(4) and 2.138(4) Å are longer than the mean Ir–O bond length of 2.088 Å reported in the Cambridge Crystallographic Database

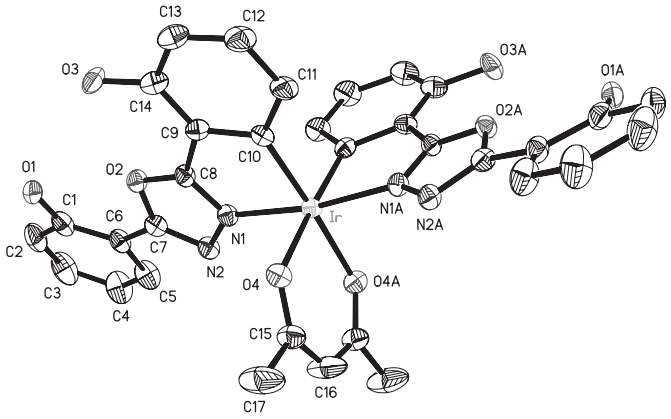

Figure 4. ORTEP figure of $(2\text{-OHOXD})_2Ir(acac)$ with 50% probability ellipsoids.

and these observations reflect the large trans influence of the phenyl groups. All other bond lengths and bond angles within the chelate ligands are analogous to the similar type of complexes.[3]

We have also used complex **1**, **2**, and **5** as dopants in the emitting layer to fabricate electroluminescent (EL) device (Fig. 5), the maximum brightness is 5430 cd/m^2 at 13 V for device **1**, 4969 cd/m^2 at 15 V for device **2**, and 2091 cd/m^2 at 15 V for device **3**. It was found that the power efficiency decreased with increasing current density for the devices as indicated in Figures 6 and 7. The luminescence efficiency of device **1** shows a maximum of 9.6 cd/A at 74.8 mA/cm^2. Then the efficiency starts to decrease with increasing current density, which can be attributed to the increasing triplet–triplet annihilation of the phosphor-bound excitons. However, even at a current density of 537 mA/cm^2, the luminescence efficiency still remains as high as 7.99 cd/A, corresponding to a 17% loss from the maximum value. We also used complexes **1** and **5** as the dopants and changed the hole blocking material, from BCP to TPBI, to fabricate devices **2** and **3**. Though the power efficiency, luminescence efficiency, and brightness of devices **2** and **3** are lower than that of device **1**, it is also observed that the decrease of the efficiency is small with increasing current density. This performance is significantly better than that of most other iridium complexes (Table 2). The results of luminescence efficiency of these devices are consistent with the study of photophysical properties.

As shown in Figure 8, the device **1** having fluoro-substituted dopant exhibits the expected blue shift as compared to that of device **2**, which was consistent with the PL investigation. The EL emission spectra matched the emission spectra of the complex in solution, which indicated that the EL emission was originated from the triplet excited states of the phosphors.

3. Conclusions

A series of new iridium complexes using 2,5-diaryl-[1,3,4]-oxadiazoles with different substituents as the ligands have been prepared and investigated their electrochemical,

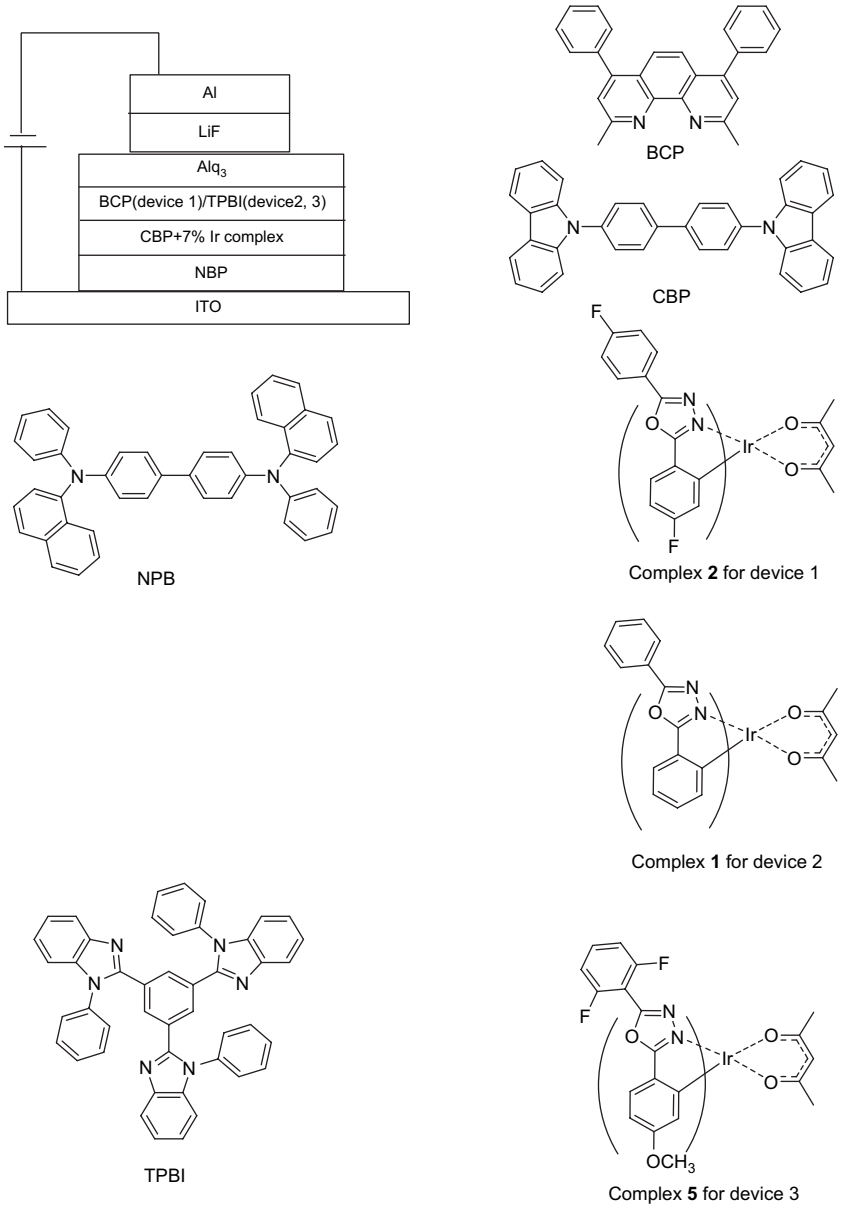

Figure 5. Schematic diagram of EL device configuration and the structures of the compounds.

photophysical, and EL properties. It is demonstrated that the emission color can be tuned depending upon different ligands. The electron-withdrawing and donating substituents on the phenyl of the OXD ligands effectively lower the HOMO levels to afford emissions with shorter wavelengths. In particular, replacement of the phenyl group by naphthyl group in 2,5-diphenyl-[1,3,4]-oxadiazole results in a red shift of the emission maxima to 569 nm. Additionally, electroluminescent devices fabricated using complexes **1**, **2**, and **5** as the phosphorescent dopants yielded efficient green-yellow emission. Especially, device **1** exhibits the best performance within the three devices, having a maximum luminescence efficiency of 9.6 cd/A at 8.5 V (J=74.8 mA/cm^2) and a maximum brightness of 5430 cd/cm^2 at 13 V. It is suggested that these complexes could be good candidates of new phosphorescent materials for OLEDs.

4. Experimental section

4.1. General

Absorption spectra were measured on a Varian Cary 500 UV–vis spectrophotometer. Fluorescence spectra were measured on a Varian Cary Eclipse Fluorescence Spectrophotometer. ^{1}H NMR spectra were recorded on a Bruker AM500 spectrometer with tetramethyl silane as internal reference. Mass spectra were obtained on a HP5989 mass spectrometer. Luminescence lifetime measurements were performed on an Edinburgh FL 900 Fluorescence Spectrometer equipped with a blue laser (λ=372 nm). The quantum efficiency (QE) measurements were carried out at room temperature in degassed THF solutions. Cyclic voltammetry was performed using an Potentiostat/Galvanostat Model K0264 (Princeton Applied

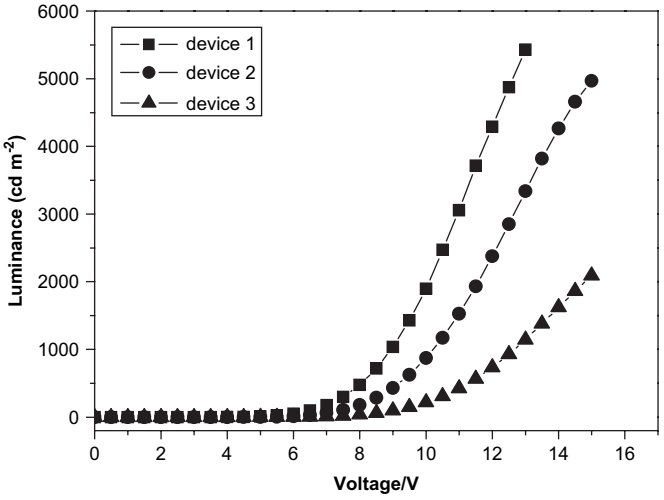

Figure 6. Luminance versus voltage characteristics of devices 1, 2, and 3.

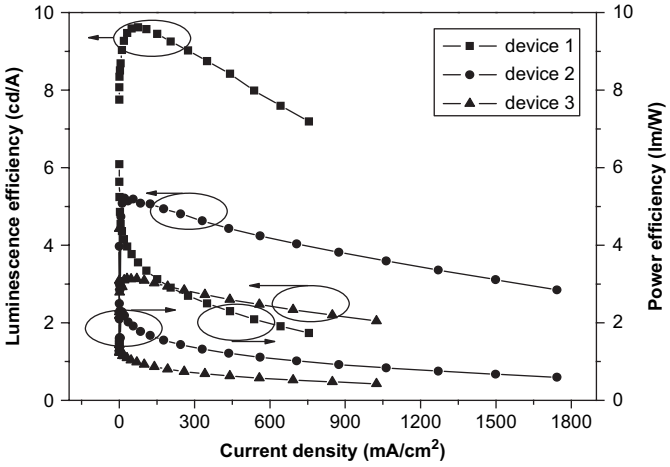

Figure 7. Current and power efficiencies of the devices 1, 2, and 3.

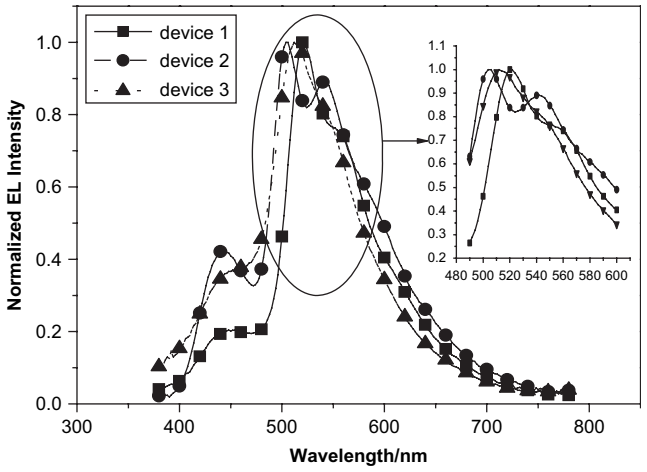

Figure 8. EL spectra of OLED devices 1, 2, and 3.

Table 3
Selected bond distances (Å) and angles (°) for $(2\text{-OHOXD})_2\text{Ir(acac)}$

Bond	Distances (Å)
Ir(1)–N(1)	2.041(5)
Ir(1)–N(1)*	2.041(5)
Ir(1)–C(10)	1.996(5)
Ir(1)–C(10)*	1.996(5)
Ir(1)–O(1)	2.116(4)
Ir(1)–O(1)*	2.116(4)
	Angles (°)
N(1)–Ir(1)–N(1)*	171.0(2)
N(1)–Ir(1)–C(10)	79.4(2)
N(1)*–Ir(1)–C(10)*	79.4(2)
N(1)–Ir(1)–O(1)	89.75(16)
C(10)*–Ir(1)–O(1)	176.03(15)
O(1)–Ir(1)–O(1)*	89.1(2)

Research). Anhydrous CH_2Cl_2 was used as the solvent under inert atmosphere, and 0.1 M tetra(*n*-butyl)ammonium perochlorate was used as the supporting electrolyte. A platinum disk electrode was used as the working electrode, a platinum wire was used as the counter electrode, and a saturated Ag/AgCl reference electrode.

A single crystal of complex **3** with the approximate dimensions $0.51\times0.36\times0.33$ mm^3 was mounted on a Rigaku RAXIS RAPID IP imaging plate system with Mo Kα radiation (λ=0.71073 Å) at 293(2) K. An empirical absorption was based on the symmetry-equivalent reflections and applied to the data using the SADABS program. The structure was solved using the SHELXL-97 program. The crystallographic refinement parameters of complex **3** are summarized in Table 2, while the selected bond distances and angles are given in Table 3.

The OLED device is fabricated on indium tin oxide (ITO) coated glass plate, which is cleaned by routine procedure including ultrasonication in detergent and de-ionized water sequentially and a final UV ozone treatment. In a vacuum chamber at a pressure of $<8\times10^{-5}$ Pa, 50 nm of NPB as the hole transporting layer, 20 nm of the complex doped (7%) CBP as the emitting layer, 10 nm of 2,9-dimethyl-4,7-diphenyl-1,10-phenanthroline (BCP) or 1,3,5-tris(2-*N*-phenylbenzimidazolyl)-benzene (TPBI) as a hole and exciton blocking layer (HBL), 40 nm of Alq_3 as the electron transporting layer, and a LiF

Table 2
Electroluminescent performance of the devices

	Device1	Device 2	Device 3
EL peak wavelength	504 nm	520 nm	511 nm
CIE-x	0.312	0.333	0.283
CIE-y	0.429	0.493	0.435
Luminance	720 cd/m^2 (at 74.8 mA/cm^2)	387 cd/m^2 (at 74.8 mA/cm^2)	238 cd/m^2 (at 74.8 mA/cm^2)
Luminescence efficiency	9.62 cd/A (at 74.8 mA/cm^2)	5.14 cd/A (at 74.8 mA/cm^2)	3.11 cd/A (at 74.8 mA/cm^2)
Power efficiency	5.24 lm/W (5 V)	2.29 lm/W (6.5 V)	1.15 lm/W (8 V)
Turn-on voltage	4 V	3 V	4.5 V

(0.7 nm)/Al (100 nm) bilayer as cathode were sequentially deposited onto the substrate to give the device structure. The current–voltage (I–V) profiles and light intensity characteristics for the above fabricated devices were measured in atmosphere at ambient temperature. The electroluminescence (EL) spectra were measured with a Spectra Scan PR705. The current–voltage (I–V) and luminance–voltage (L–V) characteristics were measured with a Keithley 236 source unit and Keithley 2000-20 multimeter with ST-86LA luminance meter.

4.2. Synthesis of oxadiazoles ligands

The oxadiazole derivatives were synthesized via a general procedure where we used the synthesis of 2,5-diphenyl-[1,3,4]-oxadiazole as an example.[7h] Benzoate (15 g, 100 mmol) was added dropwise to the ethanol solution of hydrazine monohydrate (26 g, 518 mmol) and refluxed for 17 h. Ethanol was removed under reduced pressure and the residue was poured into water. The solid was collected by filtration and then recrystallized from ethanol to yield the pure crystal product, benzohydrazide (10.6 g, 70%). Benzohydrazide (7.6 g, 50 mmol) and benzoic acid (7.5 g, 50 mmol) were dissolved in 50 mL $POCl_3$. The mixture was stirred at room temperature for 2 h and then refluxed 5 h. After cooled to room temperature, the mixture was poured into ice water carefully. The solid was collected by filtration and then recrystallized from ethanol to give the product, 2,5-diphenyl-[1,3,4]-oxadiazole, in a yield of 45% (5 g, 23 mmol).

4.3. Synthesis of iridium–oxadiazoles complexes

4.3.1. Synthesis of $(OXD)_2Ir(acac)$

All cyclometalated Ir(III) complexes were synthesized by the same method reported. The synthesis of iridium(III) bis(2,5-diphenyl)-[1,3,4]oxadiazolato-N^3,$C^{2'}$) (acetyl acetonate) ($(OXD)_2Ir(acac)$) will be described in detail. Other complexes were synthesized following in a similar procedure.

$IrCl_3\cdot 3H_2O$ (50 mg, 0.14 mmol) and 2,5-diphenyl-[1,3,4]-oxadiazole (96 mg, 0.43 mmol) were added in a 10 mL mixture of 2-ethoxyethanol and water (v/v=3:1). The mixture was refluxed for 24 h and cooled to room temperature. The solid was collected by filtration and pumped dry to give crude chloro-bridged dimer complex. Without further purification, the dimer was added in a mixture of Na_2CO_3 (88.8 mg, 0.83 mmol), acetyl acetone (5 mL), and 2-ethoxyethanol (10 mL). After refluxed for 24 h, the solution was cooled to room temperature and poured into water. The brown precipitate was filtered off and washed with water, hexane, and ether. The crude product was purified by chromatography on silica gel using CH_2Cl_2–hexane=1:1. A yellow powder was obtained with a total yield of 40%.

$(OXD)_2Ir(acac)$. Yield: 60%, ^{1}H NMR ($CDCl_3$) δ: 8.23(dd, 4H, J=4.6, 1.6 Hz), 7.59 (m, 8H), 6.98 (t, 2H, J=6.3 Hz), 6.83 (t, 2H, J=7.5 Hz), 6.72 (d, 2H, J=7.58 Hz), 5.30 (s, 1H), 1.92 (s, 6H). MS (*m/e*, ESI): 757.1 (100, M+Na^+) $C_{33}H_{25}IrN_4O_4$ (734.15) calcd C 54.01, H 3.43, N 7.64; found C 53.13, H 3.44, N 7.67.

4.3.2. Iridium(III) bis(2,5-bis-(4-fluorophenyl)-[1,3,4]oxadiazolato-$C^{2'}$,N^3) (acetyl acetonate) $(dfOXD)_2Ir(acac)$

Yield: 62%, ^{1}H NMR ($CDCl_3$) δ: 8.26 (m, 2H), 7.61 (dd, 2H, J=12.5, 3.4 Hz), 7.38 (m, 2H), 7.32 (m, 2H), 6.86 (d×d, 2H, J=13.7, 1.7 Hz), 6.62 (m, 2H), 6.45(d, 2H, J=7.6 Hz), 5.31 (s, 1H), 1.93 (s, 6H). MS (*m/e*, ESI): 829.1 (100, M+Na^+) $C_{33}H_{21}F_4IrN_4O_4$ (806.11) calcd C 49.19, H 2.63, N 6.95; found C 48.98, H 2.75, N 6.81.

4.3.3. Iridium(III) bis(2,5-bis-(2-hydroxyphenyl)-[1,3,4]oxadiazolato-$C^{2'}$,N^3) (acetyl acetonate) $(dhOXD)_2Ir(acac)$

Yield: 16%, ^{1}H NMR ($CDCl_3$) δ: 8.27 (t, 2H, J=7.4 Hz), 7.61 (m, 2H), 7.36 (m, 4H), 6.86 (d×d, 2H, J=8.7, 5.8 Hz), 6.62 (t, 2H, J=9.0 Hz), 6.45 (d, 2H, J=7.62 Hz), 5.31 (s, 1H), 1.95 (s, 6H). MS (*m/e*, ESI): 821.1 (100, M+Na^+) $C_{33}H_{25}IrN_4O_8$ (797.79) calcd C 49.68, H 3.16, N 7.02; found C 48.77, H 3.08, N 7.14.

4.3.4. Iridium(III) bis(2,5-bis-(4-methoxyphenyl)-[1,3,4]oxadiazolato-$C^{2'}$,N^3) (acetyl acetonate) $(dmOXD)_2Ir(acac)$

Yield: 72%, ^{1}H NMR ($CDCl_3$) δ: 8.13 (dd, 4H, J=7.7, 1.9 Hz), 7.51 (d, 2H, J=8.4 Hz), 7.05 (d, 4H, J=8.9 Hz), 6.48 (dd, 2H, J=8.5, 2.4 Hz), 6.19(d, 2H), 5.28 (s, 1H), 3.91(s, 6H, J=2.4 Hz), 3.62 (s, 6H), 1.91 (s, 6H). MS (*m/e*, ESI): 877.2 (100, M+Na^+) $C_{37}H_{33}IrN_4O_8$ (853.9) calcd C 52.04, H 3.90, N 6.56; found C 54.01, H 3.76, N 6.63.

4.3.5. Iridium(III) bis(2-(2,6-difluorophenyl)-5-(4-methoxyphenyl)-[1,3,4]oxadiazolato-$C^{2'}$,N^3) (acetyl acetonate) $(dfmOXD)_2Ir(acac)$

Yield: 55%, ^{1}H NMR ($CDCl_3$) δ: 8.13 (dd, 4H, J=7.7, 1.9 Hz), 7.51 (d, 2H, J=8.4 Hz), 7.05 (d, 4H, J=8.9 Hz), 6.48 (dd, 2H, J=8.5, 2.4 Hz), 6.19 (d, 2H), 5.28 (s, 1H), 3.91 (s, 6H, J=2.4 Hz), 3.62 (s, 6H), 1.91 (s, 6H). ESI: 889.1 (100, M+Na^+) $C_{33}H_{21}F_4IrN_4O_3$ calcd C 48.55, H 2.91, N 6.47; found C 47.26, H 2.85, N 6.79.

4.3.6. Iridium(III) bis(2,5-bis-(2-naphthalenyl)-[1,3,4]oxadiazolato-$C^{2'}$,N^3) (acetyl acetonate) $(nOXD)_2Ir(acac)$

Yield: 68%, ^{1}H NMR ($CDCl_3$) δ: 8.88 (s, 2H), 8.39 (dd, 2H, J=8.5, 1.5 Hz), 8.21 (s, 2H), 8.08 (d, 4H, J=5.4 Hz), 7.98 (d, 2H, J=7.6 Hz), 7.69 (m, 6H), 7.38 (d, 2H, J=7.9 Hz), 7.19 (m, 4H), 7.11 (s, 2H), 5.10 (s, 1H), 1.98 (s, 6H). MS (*m/e*, ESI): 957.2 (100, M+Na^+) $C_{49}H_{33}IrN_4O_4$ (934.03) calcd C 63.01, H 3.56, N 6.00; found C 65.04, H 3.42, N 6.02.

4.3.7. Iridium(III) bis(2,5-bis-(4-(9H-carbazol-9-yl)phenyl)-[1,3,4]oxadiazolato-$C^{2'}$,N^3) (acetyl acetonate) $(dcOXD)_2Ir(acac)$

Yield: 69%, ^{1}H NMR ($CDCl_3$) δ: 8.35 (dd, 4H, J=6.7, 1.8 Hz), 8.16 (d, 4H, J=7.8 Hz), 8.04 (d, 4H, J=7.8 Hz), 7.95 (d, 2H, J=8.1 Hz), 7.75 (d×d, 4H, J=6.7, 1.9 Hz), 7.46 (m, 8H), 7.35 (m, 12H), 7.30 (d, 2H, J=1.9 Hz), 5.44 (s,

1H), 2.05 (s, 6H). MS (*m*/*e*, ESI): 1417.5 (100, M+Na^+) $C_{33}H_{25}IrN_4O_4$ (1394.56) calcd C 69.76, H 3.83, N 8.04; found C 68.53, H 3.71, N 8.21.

Acknowledgements

Authors acknowledge the support by NSFC/China (90401026, 60508011), National Basic Research 973 Program (2006CB806200) and Scientific Committee of Shanghai. Authors thank Prof. Xiao-Yuan Hou (Dept. of Physics, Fudan University) for his help in measurements of OLEDs.

Supplementary data

Crystallographic information files for complex **3** and CV traces of all complexes were provided. Supplementary data associated with this article can be found in the online version, at doi:10.1016/j.tet.2007.11.099.

References and notes

1. (a) Baldo, M. A.; O'Brien, D. F.; You, Y.; Shoustikov, A.; Sibley, S.; Thompson, M. E.; Forrest, S. R. *Nature* **1998**, *395*, 151; (b) Yu, G.; Yin, S. W.; Liu, Y. Q.; Shuai, Z. G.; Zhu, D. B. *J. Am. Chem. Soc.* **2003**, *125*, 14816; (c) Zhao, Q.; Liu, S. J.; Shi, M.; Wang, C. M.; Yu, M. X.; Li, L.; Li, F. Y.; Yi, T.; Huang, C. H. *Inorg. Chem.* **2006**, *45*, 6152; (d) Xie, Z. Q.; Yang, B.; Li, F.; Cheng, G.; Liu, L. L.; Yang, G. D.; Xu, H.; Ye, L.; Hanif, M.; Liu, S. Y.; Ma, D. G.; Ma, Y. G. *J. Am. Chem. Soc.* **2005**, *127*, 14152.
2. (a) Holder, E.; Angeveld, B. M. W.; Schubert, U. S. *Adv. Mater.* **2005**, *17*, 1109; (b) Yin, B.; Niemeyer, F.; Williams, J. A. G.; Jiang, J.; Boucekkine, A.; Toupet, L.; Bozec, H. L.; Guerchais, V. *Inorg. Chem.* **2006**, *45*, 8584; (c) Lu, W.; Mi, B.-X.; Chan, M. C. W.; Hui, Z.; Che, C.-M.; Zhu, N.; Lee, S.-T. *J. Am. Chem. Soc.* **2004**, *126*, 4958; (d) Li, F.; Zu, Y. *Anal. Chem.* **2004**, *76*, 1768.
3. (a) Lamansky, S.; Djurovich, P.; Murphy, D.; Abdel-Razzaq, F.; Lee, H.-E.; Adachi, C.; Burrows, P. E.; Forrest, S. R.; Thompson, M. E. *J. Am. Chem. Soc.* **2001**, *123*, 4304; (b) Grushin, V. V.; Herron, N.; LeCloux, D. D.; Marshall, W. J.; Petrov, V. A.; Wang, Y. *Chem. Commun.* **2001**, 1494; (c) Ostrowski, J. C.; Robinson, M. R.; Heeger, A. J.; Bazan, G. C. *Chem. Commun.* **2002**, 784; (d) Tsuzuki, T.; Shirasawa, N.; Suzuki, T.; Tokito, S. *Adv. Mater.* **2003**, *15*, 1455; (e) Nishida, J.; Echizen, H.; Iwata, T.; Yamashita, Y. *Chem. Lett.* **2005**, *34*, 1378; (f) Yang, C.-H.; Fang, K.-H.; Chen, C.-H.; Sun, I.-W. *Chem. Commun.* **2004**, 2232; (g) Tamayo, A. B.; Alleyne, B. D.; Djurovich, P.; Lamansky, S.; Tsyba, I.; Ho, N. N.; Bau, R.; Thompson, M. E. *J. Am. Chem. Soc.* **2003**, *125*, 7377.
4. (a) Liu, Z. W.; Guan, M.; Bian, Z. Q.; Nie, D. B.; Gong, Z. L.; Li, Z. B.; Huang, C. H. *Adv. Funct. Mater.* **2006**, *16*, 1441; (b) Takizawa, S.; Echizen, H.; Nishida, J.; Tsuzuki, T.; Tokito, S.; Yamashita, Y. *Chem. Lett.* **2006**, *35*, 748; (c) Holmes, R. J.; D'Andrade, B. W.; Forrest, S. R.; Ren, X.; Li, J.; Thompson, M. E. *Appl. Phys. Lett.* **2003**, *83*, 3818; (d) Yeh, S.-J.; Wu, M.-F.; Chen, C.-T.; Song, Y.-H.; Chi, Y.; Ho, M.-H.; Hsu, S.-F.; Chen, C. H. *Adv. Mater.* **2005**, *17*, 285; (e) Tokito, S.; Iijima, T.; Suzuri, Y.; Kita, H.; Tsuzuki, T.; Sato, F. *Appl. Phys. Lett.* **2003**, *83*, 569; (f) Coppo, P.; Plummer, E. A.; De Cola, L. *Chem. Commun.* **2004**, 1774; (g) Dedeian, K.; Shi, J. M.; Shepherd, N.; Forsythe, E.; Morton, D. C. *Inorg. Chem.* **2005**, *44*, 4445.
5. (a) Jiang, C. Y.; Yang, W.; Peng, J. B.; Xiao, S.; Cao, Y. *Adv. Mater.* **2004**, *16*, 537; (b) Yang, C. H.; Tai, C. C.; Sun, I. W. *J. Mater. Chem.* **2004**, *14*, 947; (c) Duan, J. P.; Sun, P. P.; Cheng, C. H. *Adv. Mater.* **2003**, *15*, 224; (d) Niu, Y. H.; Chen, B. Q.; Liu, S.; Yip, H.; Bardecker, J.; Jen, A. K. Y.; Kavitha, J.; Chi, Y.; Shu, C. F.; Tseng, Y. H.; Chien, C. H. *Appl. Phys. Lett.* **2004**, *85*, 1619; (e) Takizawa, S.-Y.; Nishida, J.-I.; Tsuzuki, T.; Tokito, S.; Yamashita, Y. *Inorg. Chem.* **2007**, *46*, 4308.
6. Chen, L. Q.; You, H.; Yang, C. L.; Ma, D. G.; Qin, J. G. *Chem. Commun.* **2007**, 1352.
7. (a) Brunner, K.; Dijken, A. V.; Borner, H.; Bastiaansen, J. J. A. M.; Kiggen, N. M. M.; Langeveld, B. M. W. *J. Am. Chem. Soc.* **2004**, *126*, 6035; (b) Ma, W.; Iyer, P. K.; Gong, X.; Liu, B.; Moses, D.; Bazan, G. C.; Heeger, A. J. *Adv. Mater.* **2005**, *17*, 274; (c) Wang, C.; Jung, G. Y.; Hua, Y.; Pearson, C.; Bryce, M. R.; Petty, M. C.; Batsanov, A. S.; Goeta, A. E.; Howard, J. A. K. *Chem. Mater.* **2001**, *13*, 1167; (d) Zhan, X.; Liu, Y.; Wang, S. W.; Zhu, D. *Macromolecules* **2002**, *35*, 2529; (e) Lee, Y. Z.; Chen, X.; Chen, S. A.; Wei, P. K.; Fann, W. S. *J. Am. Chem. Soc.* **2001**, *123*, 2296; (f) Chung, S. J.; Kwon, K. Y.; Lee, S. W.; Jin, J. L.; Lee, C. H.; Lee, C. E.; Park, Y. *Adv. Mater.* **1998**, *10*, 1112; (g) Kim, J. H.; Park, J. H.; Lee, H. *Chem. Mater.* **2003**, *15*, 3414; (h) Zhu, W. H.; Yao, R.; Tian, H. *Dyes Pigments* **2002**, *54*, 147–154.
8. Jung, S. G.; Kang, Y. J.; Kim, H.-S.; Kim, Y.-H.; Lee, C.-L.; Kim, J.-J.; Lee, S.-K.; Kwon, S.-K. *Eur. J. Inorg. Chem.* **2004**, *17*, 3415.
9. Laskar, I. R.; Chen, T.-M. *Chem. Mater.* **2004**, *16*, 111.
10. (a) Li, Y.; Ding, J.; Day, M.; Tao, Y.; Lu, J.; D'iorio, M. *Chem. Mater.* **2004**, *16*, 2165; (b) Ding, J.; Gao, J.; Cheng, Y.; Xie, Z.; Wang, L.; Ma, D.; Jing, X.; Wang, F. *Adv. Funct. Mater.* **2006**, *16*, 575; (c) Loiseau, F.; Campagna, S.; Hameurlaine, A.; Dehaen, W. *J. Am. Chem. Soc.* **2005**, *127*, 11352.
11. Xie, H. Z.; Liu, M. W.; Wang, O. Y.; Zhang, X. H.; Lee, C. S.; Hung, L. S.; Lee, S. T.; Teng, P. F.; Kwong, H. L.; Zheng, H.; Che, C. M. *Adv. Mater.* **2001**, *13*, 1245.